Phase discrimination and simultaneous frequency conversion of the orthogonal components of an optical signal by four-wave mixing in an SOA

R. P. Webb,* J. M. Dailey, R. J. Manning and A. D. Ellis

Tyndall National Institute & Department of Physics, University College Cork, Lee Maltings, Cork, Ireland
*rod.webb@tyndall.ie

Abstract: Simultaneous conversion of the two orthogonal phase components of an optical input to different output frequencies has been demonstrated by simulation and experiment. A single stage of four-wave mixing between the input signal and four pumps derived from a frequency comb was employed. The nonlinear device was a semiconductor optical amplifier, which provided overall signal gain and sufficient contrast for phase sensitive signal processing. The decomposition of a quadrature phase-shift keyed signal into a pair of binary phase-shift keyed outputs at different frequencies was also demonstrated by simulation.

References and links

1. K. N. Nguyen, T. Kise, J. M. Garcia, H. Poulsen, and D. J. Blumenthal, "All-optical 2R regeneration of BPSK and QPSK data using a 90° optical hybrid and integrated SOA-MZI wavelength converter pairs," in *Optical Fiber Communication Conference*, OSA Technical Digest (CD) (Optical Society of America, 2011), paper OMT3.
2. Z. Zheng, L. An, Z. Li, X. Zhao, J. Yan, and X. Liu, "All-optical regeneration of DQPSK/QPSK signals based on phase-sensitive amplification," in *Optical Fiber Communication Conference and Exposition and The National Fiber Optic Engineers Conference*, OSA Technical Digest (CD) (Optical Society of America, 2008), paper JWA71.
3. J. Kakande, A. Bogris, R. Slavik, F. Parmigiani, D. Syvridis, P. Petropoulos, and D. J. Richardson, "First demonstration of all-optical QPSK signal regeneration in a novel multi-format phase sensitive amplifier," in *2010 36th European Conference and Exhibition on Optical Communication (ECOC)* (2010), postdeadline paper 3.3, pp. 1-3.
4. J. Kakande, A. Bogris, R. Slavik, F. Parmigiani, D. Syvridis, P. Petropoulos, D. Richardson, M. Westlund, and M. Sköld, "QPSK phase and amplitude regeneration at 56 Gbaud in a novel idler-free non-degenerate phase sensitive amplifier," in *Optical Fiber Communication Conference*, OSA Technical Digest (CD) (Optical Society of America, 2011), paper OMT4.
5. R. Tang, J. Lasri, P. S. Devgan, V. Grigoryan, P. Kumar, and M. Vasilyev, "Gain characteristics of a frequency nondegenerate phase-sensitive fiber-optic parametric amplifier with phase self-stabilized input," Opt. Express **13**(26), 10483–10493 (2005).
6. R. Slavík, F. Parmigiani, J. Kakande, C. Lundström, M. Sjödin, P. A. Andrekson, R. Weerasuriya, S. Sygletos, A. D. Ellis, L. Grüner-Nielsen, D. Jakobsen, S. Herstrøm, R. Phelan, J. O'Gorman, A. Bogris, D. Syvridis, S. Dasgupta, P. Petropoulos, and D. J. Richardson, "All-optical phase and amplitude regenerator for next-generation telecommunications systems," Nat. Photonics **4**(10), 690–695 (2010).
7. W. Imajuku, A. Takada, and Y. Yamabayashi, "Low-noise amplification under the 3 dB noise figure in high-gain phase-sensitive fibre amplifier," Electron. Lett. **35**(22), 1954–1955 (1999).
8. Y. Leng, C. J. Richardson, and J. Goldhar, "Phase-sensitive amplification using gain saturation in a nonlinear Sagnac interferometer," Opt. Express **16**(26), 21446–21455 (2008).
9. K. A. Croussore and G. Li, "Phase-regenerative wavelength conversion for BPSK and DPSK signals," IEEE Photon. Technol. Lett. **21**(2), 70–72 (2009).
10. S. Haykin and M. Moher, *Analog & Digital Communications*, 2nd ed. (Wiley, 2007).

11. G. Talli and M. Adams, "Gain dynamics of semiconductor optical amplifiers and three-wavelength devices," IEEE J. Quantum Electron. **39**(10), 1305–1313 (2003).
12. G. Talli and M. Adams, "Amplified spontaneous emission in semiconductor optical amplifiers: modelling and experiments," Opt. Commun. **218**(1–3), 161–166 (2003).
13. J. Leuthold, M. Mayer, J. Eckner, G. Guekos, H. Melchior, and C. Zellweger, "Material gain of bulk 1.55 μm InGaAsP/InP semiconductor optical amplifiers approximated by a polynomial model," J. Appl. Phys. **87**(1), 618–620 (2000).
14. J. A. Nelder and R. Mead, "A simplex method for function minimization," Comput. J. **7**, 308–313 (1965).
15. C. F. C. Silva, A. J. Seeds, and P. J. Williams, "Terahertz span >60-channel exact frequency dense WDM source using comb generation and SG-DBR injection-locked laser filtering," IEEE Photonics Technol. Lett. IEEE **13**(4), 370–372 (2001).
16. W. Mao, P. A. Andrekson, and J. Toulouse, "Investigation of a spectrally flat multi-wavelength DWDM source based on optical phase- and intensity-modulation," in *Optical Fiber Communication Conference*, Technical Digest (CD) (Optical Society of America, 2004), paper MF78.
17. G. Maxwell, A. Poustie; C. Ford, M. Harlow, P. Townley, M. Nield, T. Lealman, S. Oliver, L. Rivers, and R. Waller, "Hybrid integration of monolithic semiconductor optical amplifier arrays using passive assembly," in *55th Electronic Components and Technology Conference, 2005. Proceedings* (2005), Vol. 2, pp. 1349–1352.

1. Introduction

Four-wave mixing in nonlinear optical devices is a well-known mechanism for the phase-sensitive amplification or frequency conversion of signals, two processes that have important applications in telecommunications. Here it is shown, by both simulation and experiment, that an input signal can be separated into two phase components and simultaneously frequency converted by mixing the signal with a four-tooth frequency comb as the pumps. The signal can, in effect, be resolved with high contrast into orthogonal phasors, each of which is converted to a different output frequency. Thus, as confirmed in a further simulation, a quadrature phase-shift keyed (QPSK) signal can be separated, or demultiplexed, into two binary phase-shift keyed (BPSK) outputs. Decomposition of QPSK is normally accomplished by a coherent receiver which converts the orthogonal phase components into a pair of electrical signals, but in this scheme the output signals remain in the optical domain. The signals could, for example, be separated at a network branch point for onward transmission to different destinations. Converting the modulation format to BPSK generates signals that have the advantage of being simpler to detect, each requiring only a single-bit delay interferometer and a direct-detection receiver. Resolving the signal into its orthogonal components could also serve as the phase regeneration stage in an all-optical QPSK regenerator [1–4].

One type of phase-sensitive amplifier (PSA), suitable for BPSK signals, employs two pumps with frequencies symmetrically placed about the signal frequency [5,6]. It has recently been shown that phase-sensitive amplification of QPSK signals is also possible by using an asymmetrically placed pair of pumps to create a four-step phase transfer response [3,4]. With either arrangement, the mixing products generated at the signal frequency only add constructively and enhance the signal when the signal and the pumps have the correct phase relationship. In general, phase selectivity requires the signal to beat with more than one pump (unless the pump and signal share the same frequency [7,8]). Frequency conversion using four-wave mixing can also be made phase sensitive if multiple pumps are employed [9]. Phase discrimination is potentially greater in a frequency converter than in a frequency-maintaining PSA, because the original signal can be filtered out.

2. Principle

In the scheme reported here, four pumps form a phase-locked frequency comb with spacing $2\Delta f$ (i.e. with frequencies $-3\Delta f$, $-\Delta f$, $+\Delta f$ and $+3\Delta f$ relative to the comb center). The frequency of the input signal is midway between the two highest pump frequencies (i.e. at $+2\Delta f$). Mixing in a nonlinear device generates many modulation products with Δf frequency spacing (Fig. 1a). The signals produced between the central pair of pumps and between the lowest frequency pair are chosen as the outputs (0 and $-2\Delta f$). By choosing the appropriate powers and phases for the pumps, these outputs can be made to vary in proportion to the orthogonal

phase components of the signal. Furthermore, if the signal is modulated with the QPSK format, the outputs become modulated with the two BPSK signals into which it may be decomposed. (Gray code QPSK is identical to 4QAM and is the sum of two orthogonal input signals [10].) In a coherent receiver, a 90° hybrid optical coupler followed by differential detectors is used to convert QPSK into two electrical signals. Here, the outputs take the form of optical signals separated in frequency. As with coherent detection, phase locking is required, in this case between the signal and the pump comb.
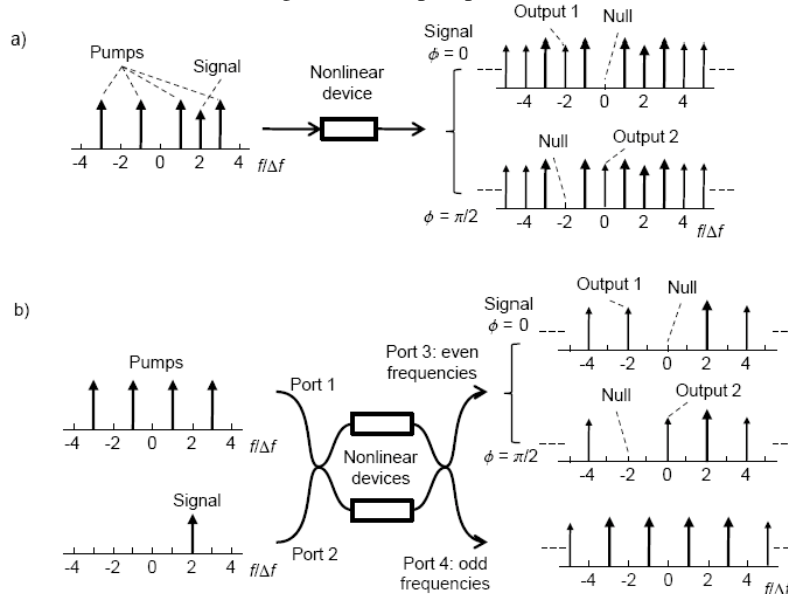

Fig. 1. Proposed scheme showing input and output spectra. a) With a single nonlinear device. Signal and pumps have been combined in a preceding coupler. b) With a pair of nonlinear devices in an MZI showing separation of the output signals from the amplified pumps. Nonlinear fiber could equivalently be incorporated in a Sagnac interferometer.

The nonlinear optical mixing elements used in this work were semiconductor optical amplifiers (SOAs), which are rarely employed in phase-sensitive applications [8], but it is likely that other nonlinear devices could produce similar results. The use of SOAs here provided overall signal gain and sufficient contrast for phase sensitive signal processing while requiring only sub-milliwatt input powers and avoiding problems caused by stimulated Brillouin scattering (SBS). In an alternative arrangement (Fig. 1b), a pair of nonlinear devices is placed in the arms of a symmetrical Mach-Zehnder interferometer (MZI), which is equivalent to the use of a Sagnac interferometer in the single-pump degenerate PSA [7,8]. The advantage is that the two output signals and other modulation products generated at even multiples of Δf appear at one output port, while the products at odd multiples of Δf, including the amplified pumps, appear at the other. The demands placed on the output filters are consequently eased. An additional benefit is that both arms of the input coupler are used and so none of the input signal or pump power is lost.

3. Implementation and results

The version of the scheme shown in Fig. 1a was tested using a continuous tone with variable phase as the input signal, firstly by simulation and secondly by experiment. Then a further simulation with the arrangement shown in Fig. 1b was carried out using a QPSK-modulated input signal.

3.1. Simulation with a CW input signal

The SOA was simulated by a multi-section time-domain model of the carrier dynamics within the device, similar to that described in [11,12], but with the following additional features. The temporal and longitudinal variations of the carrier temperature in response to the internal optical power levels were calculated using rate equations similar to those used to represent the carrier density. The approximation to the gain spectrum introduced in [13] was employed to enable the gain and ASE spectra to be represented efficiently as functions of both time and distance along the SOA. The main parameters of the simulated device are shown in Table 1.

Table 1. SOA parameters used for simulation

| Bias current	I	400mA	Waveguide loss	γ	2.3×10^3 m^{-1}
Cross-section area	A	2.0×10^{-13} m^2	Optical confinement	Γ	0.18
Length	L	2.2mm	α parameter: bandfilling	α_{BF}	5.7
Transparency density	N_0	5.3×10^{23} m^{-3}	carrier heating	α_{CH}	1.5
Recombination coefficients: non-radiative	a_s	2.2×10^8 s^{-1}	Equiv. density reduction for carrier temperature rise	dN/dT	3.3×10^{21} m^{-3}K^{-1}
spontaneous emission	b_s	2.0×10^{-16} m^{3}s^{-1}	Carrier cooling time	τ_{CH}	1ps
Auger	c_s	6.3×10^{-40} m^{6}s^{-1}	Unsaturated gain peak	λ_{PK}	1564nm
Material gain coefficient	a	3.8×10^{-20} m^2			
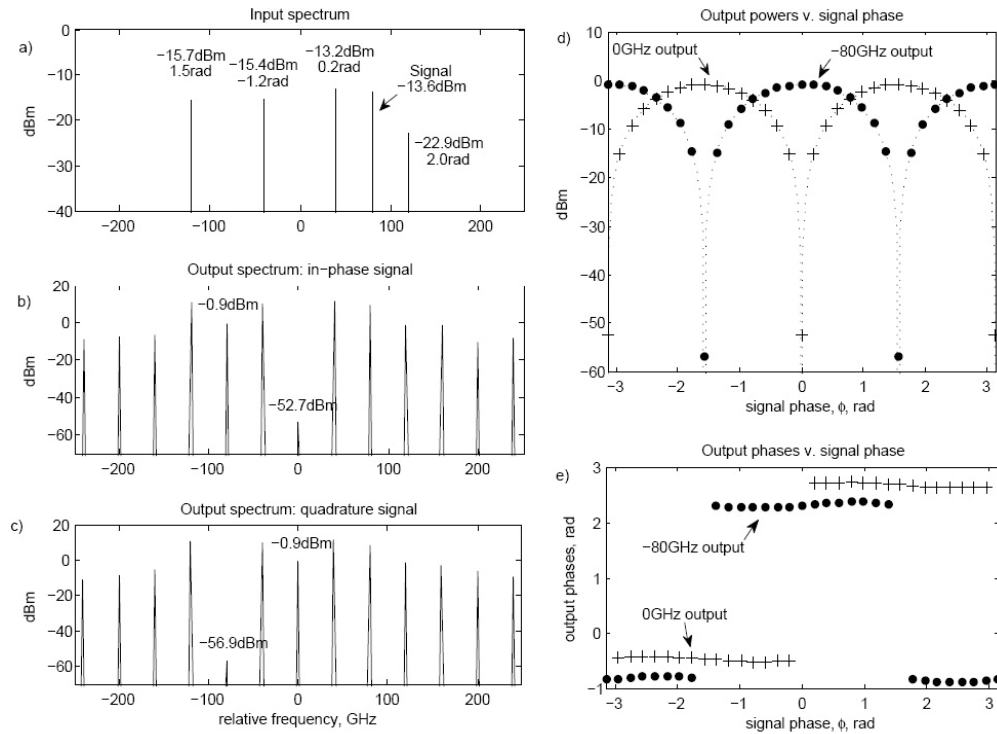
Fig. 2. Simulation results with CW input signal. a) Input spectrum showing signal and pumps with optimized powers and phases. b) Output spectrum for in-phase signal ($\phi = 0$). c) Output spectrum for quadrature signal ($\phi = \pi/2$). d) The output powers at 0 and −80GHz (symbols) varied with signal phase in proportion to $\sin^2\phi$ and $\cos^2\phi$ respectively (dotted lines).e) The output phases at 0 and −80GHz showed step responses to signal phase.

The pump inputs constituted an 80GHz-spaced frequency comb with four "teeth" (spectral lines) centered on a reference frequency of 192THz (1560nm). The input signal was placed at

+ 80GHz, midway between two of the comb teeth (Fig. 2a). These five inputs were combined to form a complex equivalent-baseband time-domain input to the SOA model. The output of the simulation was Fourier transformed to obtain the output spectrum. The output frequencies were defined as −80 and 0GHz relative to the reference frequency, the centres of the two remaining gaps in the pump comb. An optimisation routine based on the Nelder-Mead simplex method [14] was used to adjust the powers and phases of the pump inputs to maximize the variation of these output signals as the input signal phase was changed from $\phi = 0$ to $\phi = \pi/2$.

When the optimization was complete, the SOA output spectra for the two orthogonal input signal phases were calculated. For $\phi = 0$, the power of the −80GHz output was −0.9dBm while the 0GHz output was suppressed by more than 50dB (Fig. 2b). Conversely, for $\phi = \pi/2$, the power of the 0GHz output rose to −0.9dBm while the −80GHz output was in turn suppressed by more than 50dB (Fig. 2c).

Retaining the optimized pump settings, the input signal phase was varied in steps from -π to π and the powers and phases of the two outputs were recorded. The output powers varied in proportion to $\cos^2\phi$ and $\sin^2\phi$ (Fig. 2d) and the output phases approximated the step response of an ideal phase regenerator (Fig. 2e). It follows that the output fields were proportional to $\cos\phi$ and $\sin\phi$, the orthogonal components of the input signal.

3.2. Experiment with a CW input signal

The scheme shown in Fig. 1a was tested experimentally by generating a frequency comb with individually variable teeth, passing it through a nonlinear SOA and observing the result on an optical spectrum analyzer. A mode locked semiconductor laser (u^2t Picosecond Laser Source) driven by a 42.6GHz RF input provided a comb, which was passed through a programmable filter (Finisar Waveshaper 1000s) configured to control the amplitude and phase of each tooth. The teeth with frequencies ± 42.6 and ± 127.8GHz relative to the central tooth at 192.8THz (1555nm) were used as the four pumps and the tooth at + 85.2GHz was used as the signal (Fig. 3a). Other teeth in the comb were attenuated by approximately 50dB. Signal and pumps mixed in a nonlinear SOA (NL OEC 1550 from CIP Technologies) with the properties listed in Table 2.

Table 2. Properties of experimental SOA

Type	SOA-NL-OEC-1550
Structure	InP buried heterostructure
Bias current	400mA
Unsaturated gain peak wavelength	1560nm
Small signal gain	30dB
Saturated output power	8dBm

Spectra were recorded with the phase of the input signal, ϕ, set to 0 and $\pi/2$ radians by the programmable filter. The lines generated at relative frequencies 0 and −85.2GHz were used as the outputs. The amplitudes and phases of the pumps were optimized to maximize the differences between the two output signals, using the same algorithm employed in the simulations. The pump and signal powers measured in the SOA input fiber and the programmable filter phase settings are given in Fig. 3a. Following the optimization, the 0GHz output reached −2.5dBm for the in-phase input signal, $\phi = 0$ radians, and the −85.2GHz output was −8.3dBm for the quadrature input signal, $\phi = \pi/2$ radians (Figs. 3b, c). These output powers represent gains of 10.6dB and 4.8dB, respectively, relative to the input signal level. In each case, the unwanted output signal was 26dB less than the wanted output.

Following a second optimization that yielded similar results, the input signal phase was stepped from -π to +π and the two output powers were recorded (Fig. 3d). In the experiments, the relationship between the output powers and the input phase took the opposite sense to the

results of the simulations, but this could easily be modified by the appropriate choice of overall phase reference. In this case, the 0 and −85.2GHz outputs were approximately proportional to $\cos^2\phi$ and $\sin^2\phi$ respectively. (The 0GHz output also showed a gradual increase during the course of the measurement.) This result is consistent with the input signal being resolved into its in-phase and quadrature components.
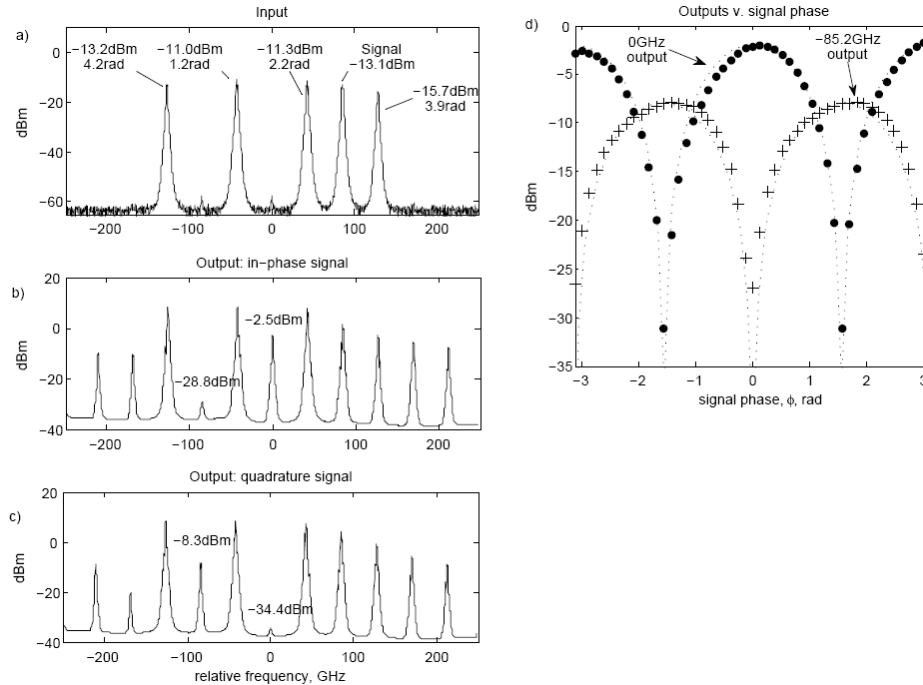

Fig. 3. Experimental results with CW input signal. a) Input spectrum showing signal and pumps with optimized powers. The phases shown are the programmable filter settings. b) Output spectrum for in-phase signal ($\phi = 0$). c) Output spectrum for quadrature signal ($\phi = \pi/2$). d) The output powers at 0 and −85.2GHz (symbols) varied approximately in proportion to $\cos^2\phi$ and $\sin^2\phi$ respectively (dotted lines).

3.3. Simulation with a QPSK input signal

A further simulation was carried out to investigate the operation of the scheme with a modulated signal. The arrangement with a nonlinear SOA in each arm of an MZI was used in order to remove the pump lines from the output (Fig. 4). The signal and the pump comb had
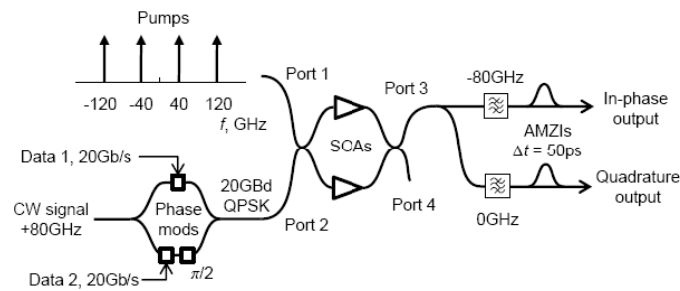

Fig. 4. QPSK simulation system. The frequencies shown are relative to the pump comb center frequency, 192THz (1560nm). AMZI = asymmetric Mach-Zehnder interferometer.

the same frequencies as for the previous simulation, but were connected to different input ports of the MZI. Two 128-bit random bit sequences were used to generate a 20GBd RZ

QPSK-modulated signal. The SOA parameters were the same as for the previous simulation (Table 1). The in-phase and quadrature output signals were extracted by 41GHz (full-width 3dB bandwidth) elliptical filters centered on the relative frequencies −80 and 0GHz, respectively. The two BPSK output signals were differentially demodulated by single-bit delay interferometers to obtain amplitude modulated signals. (Coherent detection would have exaggerated the phase discrimination.) Pump powers and phases were optimized for the best quality output eyes (Fig. 5a).

The output spectrum before the filters showed that the four-wave mixing process had generated many mixing products carrying the signal modulation (Fig. 5b). In general, they contained components originating from both the in-phase and quadrature constituents of the
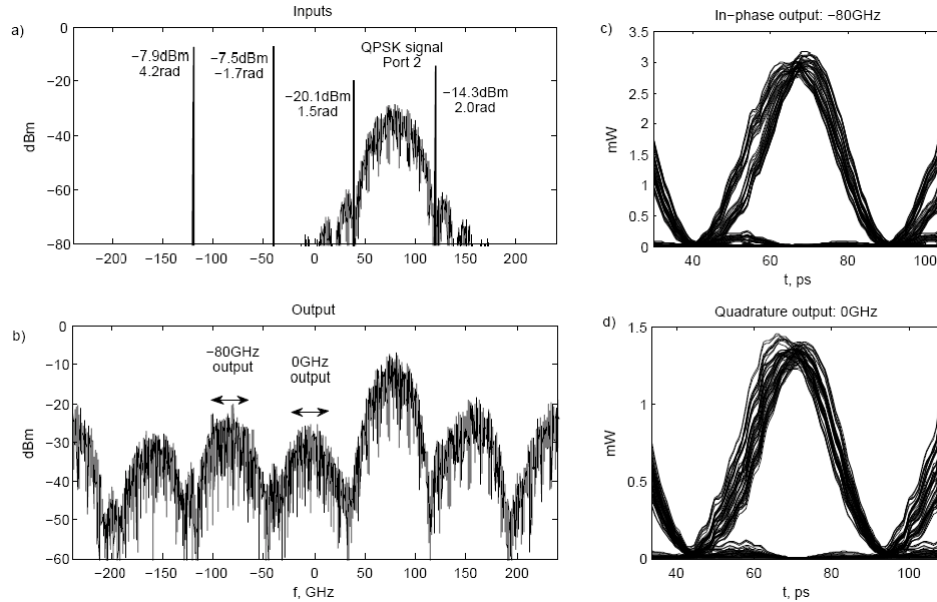

Fig. 5. Simulation results with QPSK input signal. a) Composite input spectrum showing pumps with optimized powers and phases applied to port 1 and the 20GBd QPSK signal applied to port 2. b) Output spectrum at port 3. c) Eye diagram of demodulated in-phase signal. d) Eye diagram of demodulated quadrature signal.
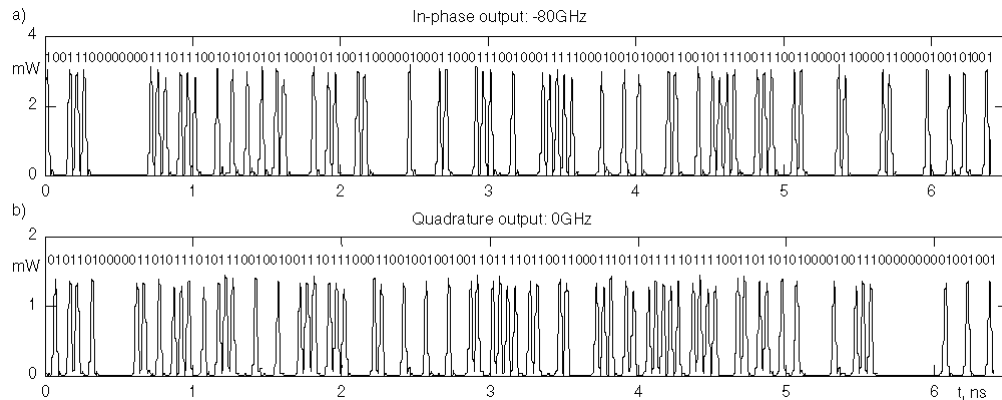

Fig. 6. Demodulated waveforms: a) In-phase output at −80GHz, b) Quadrature output at 0GHz. The binary streams show the two 128-bit input data sequences after differential decoding.

signal, except for the two outputs which had been optimized for phase discrimination. The pump comb was suppressed by the MZI.

Following the filters and demodulators, the mean powers of the in-phase and quadrature outputs were −2.0dBm and −4.8dBm respectively. Both output eyes showed very low crosstalk (Figs. 5c, d) and comparison of the output waveforms with the differentially decoded input data showed that there were no bit-errors (Fig. 6).

4. Discussion

The experimental spectra (Figs. 3b, c) show that for orthogonal input signal phases, the unwanted output was 26dB below the wanted output. However, there was a 6dB difference in the peak powers reached by each output (Fig. 3d), which gave rise to an asymmetry in the extinction achieved at each output as the signal phase was varied. The extinction at the in-phase output was 32dB, whereas at the quadrature output it was limited to 20dB. These values represent the potential level of crosstalk from the orthogonal phase and are believed to be more than adequate for phase sensitive signal processing. However, the Nelder-Mead optimization algorithm [14] is intended to operate on a function free of random variations. In the experiment, the optimization of the pumps appeared to have been restricted by the repeatability of the spectral measurements, which, together with the better results obtained in simulation, suggests that further improvements are possible.

Implementation of the scheme requires only readily available photonic components. The pump comb may either be derived from a mode-locked laser, as in the experiment described above, or alternatively obtained by RF modulation of a CW source [15,16]. Narrower linewidths are normally achievable with the latter technique. An arrayed waveguide grating could be used as the programmable filter or a planar lightwave circuit consisting of interleavers and phase shifters could be developed. Integrated MZIs incorporating nonlinear SOAs are already mature components [17].

5. Conclusions

These results show that the known uses of four-wave mixing for phase sensitive amplification and phase sensitive frequency conversion may be extended to the simultaneous conversion of the orthogonal phase components of an input signal to separate frequencies. The use of an SOA enabled the nonlinear mixing to be carried out at low input powers, with gain and free from SBS. The simulation and experiment with a CW input signal showed high contrast between the outputs corresponding to the in-phase and quadrature input phases. The variation of these outputs in proportion to $\cos^2\phi$ and $\sin^2\phi$ as the input phase, ϕ, was varied implied that the signal was being resolved into its orthogonal components. This was confirmed by the QPSK simulation which showed that the modulated signal could be separated into two BPSK signals with low crosstalk. Consequently, QPSK and other higher level modulation schemes can now be regarded as multiplexing formats that may be readily phase-demultiplexed into a pair of constituent signals. The almost ideal regenerative input phase to output phase characteristic obtained in the simulation suggests that the scheme could be exploited in a QPSK regenerator.